Coherence patterns originating from incoherent volume sources

Kehan Tian and George Barbastathis

Department of Mechanical Engineering, Massachusetts Institute of Technology, Room 3-461c, 77 Massachusetts Avenue, Cambridge, Massachusetts 02139

Received October 6, 2003

We derive the complex degree of coherence that originates from generalized incoherent two- and three-dimensional sources. Further, we find the locus of maximum coherence and analyze the dependence of the decay of coherence on source thickness.

OCIS codes: 030.1640, 030.1670, 060.2370, 290.5850.

Fast-spinning random phase masks are often used to make the behavior of light sources that are inherently spatially coherent (e.g., a monochromatic laser source) emulate spatially incoherent behavior. The coherence pattern generated by such a source can be well characterized by the Airy function[1,2] on a plane perpendicular to the optical axis. Here we derive the off-plane behavior of the coherence function for two-dimensional (such as a spinning disk) and three-dimensional generalized incoherent sources. We find that maximum coherence off plane is obtained along radial lines that diverge from the source center, branching out at certain locations. The decay of coherence as a function of source thickness is also characterized.

Consider a field in the half-space $z > 0$ originating from a quasi-monochromatic, spatially incoherent volume source, as shown in Fig. 1. Mutual intensity $J(\mathbf{r}_1', \mathbf{r}_2')$ of the field at any two points $P'(\mathbf{r}_1')$ and $Q'(\mathbf{r}_2')$ within source volume $\mathcal{V}$ is

$$J(\mathbf{r}_1', \mathbf{r}_2') = I(\mathbf{r}_1')\delta(\mathbf{r}_2' - \mathbf{r}_1'). \tag{1}$$

The complex degree of coherence of the field at any pair of points $P(\mathbf{r}_1)$ and $Q(\mathbf{r}_2)$ in half-space $z > 0$ past the source is[1,2]

$$j(\mathbf{r}_1, \mathbf{r}_2) = \frac{1}{[I_0(\mathbf{r}_1)]^{1/2}[I_0(\mathbf{r}_2)]^{1/2}} \iiint_{\mathcal{V}} I(\mathbf{r}_1') \times \frac{\exp[\,j(2\pi/\lambda)|\mathbf{r}_1 - \mathbf{r}_1'|]}{j\lambda|\mathbf{r}_1 - \mathbf{r}_1'|} \times \frac{\exp[-j(2\pi/\lambda)|\mathbf{r}_2 - \mathbf{r}_1'|]}{-j\lambda|\mathbf{r}_2 - \mathbf{r}_1'|} \mathrm{d}^3\mathbf{r}_1', \tag{2}$$

where

$$I_0(\mathbf{r}_i) = \frac{1}{\lambda^2} \iiint_{\mathcal{V}} \frac{I(\mathbf{r}_1')}{|\mathbf{r}_i - \mathbf{r}_1'|^2} \mathrm{d}^3\mathbf{r}_1'. \tag{3}$$

Consider the geometry in Fig. 1 again. We are interested in the degree of coherence between point $P(\mathbf{r}_1)$ at reference plane Π_1 located a distance z_1 from the coordinate origin and point $Q(\mathbf{r}_2)$ located at a different plane, Π_2. Δz is the distance between the two planes. Assuming that the paraxial approximation is valid for both $P(\mathbf{r}_1)$ and $Q(\mathbf{r}_2)$, Eq. (2) can be written as

$$j(\mathbf{r}_1, \mathbf{r}_2) \approx \frac{\exp[-j(2\pi/\lambda)\Delta z]}{\lambda^2 z_1(z_1 + \Delta z)[I_0(\mathbf{r}_1)I_0(\mathbf{r}_2)]^{1/2}} \iiint_{\mathcal{V}} \times I(x_1', y_1', z_1')\exp[\,j\pi A(z_1')(x_1'^2 + y_1'^2)] \times \exp\{\,j2\pi[B_x(z_1')x_1' + B_y(z_1')y_1']\} \times \exp[\,j\pi C(z_1')]\mathrm{d}x_1'\mathrm{d}y_1'\mathrm{d}z_1'. \tag{4}$$

Coefficients $A(z_1')$, $B_x(z_1')$, $B_y(z_1')$, and $C(z_1')$ are expressed as

$$A(z_1') = \frac{1}{\lambda(z_1 - z_1')} - \frac{1}{\lambda(z_1 + \Delta z - z_1')}, \tag{5}$$

$$B_x(z_1') = -\frac{1}{\lambda}\left(\frac{x_1}{z_1 - z_1'} - \frac{x_2}{z_1 + \Delta z - z_1'}\right), \tag{6}$$

$$B_y(z_1') = -\frac{1}{\lambda}\left(\frac{y_1}{z_1 - z_1'} - \frac{y_2}{z_1 + \Delta z - z_1'}\right), \tag{7}$$

$$C(z_1') = \frac{{x_1}^2 + {y_1}^2}{\lambda(z_1 - z_1')} - \frac{{x_2}^2 + {y_2}^2}{\lambda(z_1 + \Delta z - z_1')}. \tag{8}$$

The special case when the source is a cylinder of radius R and thickness L centered at the coordinate origin with uniform intensity is shown in Fig. 2. We introduce Fresnel number $N_F = R^2/\lambda z_1$ (Ref. 3) and thickness/distance ratio $\alpha = L/z_1$ and express all

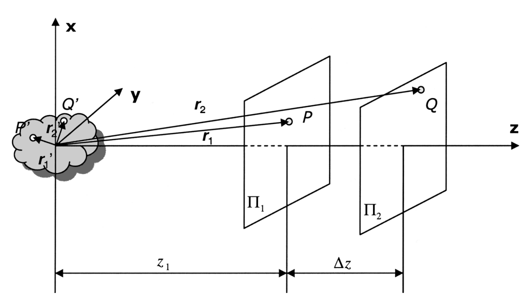

Fig. 1. Illustration of the coherence that originates from a quasi-monochromatic, spatially incoherent volume source.

0146-9592/04/070670-03$15.00/0

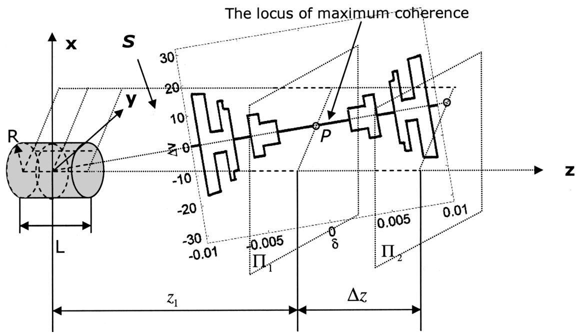

Fig. 2. Illustration of the coherence that originates from a cylindrical, quasi-monochromatic, spatially incoherent source: The parameters that we used to calculate the locus of maximum coherence are $\lambda = 488$ nm, $R = 5$ mm, $L = 10$ mm, and $\mathbf{r}_1 = (10, 10, 100 \text{ mm})$, which led to $N = 512.3$, $\alpha = 0.1$, $v_{x_1} = 6437.7$, and $v_{y_1} = 6437.7$.

distances in dimensionless units as

$$\eta_x = x_1'/R\,, \qquad \eta_y = y_1'/R\,, \qquad \xi = z_1'/z_1\,,$$
$$\delta = \Delta z/z_1\,, \qquad v_{x_1} = \frac{2\pi}{\lambda}\frac{R}{z_1}x_1\,, \qquad v_{y_1} = \frac{2\pi}{\lambda}\frac{R}{z_1}y_1\,,$$
$$v_1 = \sqrt{{v_{x_1}}^2 + {v_{y_1}}^2}\,, \qquad v_{x_2} = \frac{2\pi}{\lambda}\frac{R}{z_1}x_2\,,$$
$$v_{y_2} = \frac{2\pi}{\lambda}\frac{R}{z_1}y_2\,, \qquad v_2 = \sqrt{{v_{x_2}}^2 + {v_{y_2}}^2}\,. \tag{9}$$

Then expression (4) can be integrated explicitly in cylindrical coordinates, leading to

$$j(\mathbf{r}_1, \mathbf{r}_2) = \frac{\exp[-j(2\pi/\lambda)\Delta z]}{\alpha}\int_{-\alpha/2}^{\alpha/2}\exp[j\pi C(\xi)] \times \mathcal{L}[2\pi A(\xi), 2\pi B(\xi)]\mathrm{d}\xi\,, \tag{10}$$

where $B(\xi) = [B_x(\xi)^2 + B_y(\xi)^2]^{1/2}$ and $\mathcal{L}()$ is a function that also describes the three-dimensional field distribution in the focal vicinity of an ideal lens.[4] The derivation is similar to that which is used to obtain the field diffracted from a volume hologram.[5] Modulus $|j(\mathbf{r}_1, \mathbf{r}_2)|$ indicates how coherent the two points $P(\mathbf{r}_1)$ and $Q(\mathbf{r}_2)$ are with respect to each other. A straightforward deduction from Eq. (10) is in the limit $\alpha \to 0$, i.e., a disk source that can be emulated by a laser source and a spinning random phase mask in the laboratory.[2] The result is

$$j(\mathbf{r}_1, \mathbf{r}_2) = \exp\left(-j\frac{2\pi}{\lambda}\Delta z\right)\exp[j\pi C(0)] \times \mathcal{L}[2\pi A(0), 2\pi B(0)]\,. \tag{11}$$

Then Eq. (10) has an interesting interpretation. Because $\mathcal{L}()$ describes the complex degree of coherence from a disk source, Eq. (10) means that the complex degree of coherence from the cylinder volume is the coherent superposition of many disk sources stacked in the z direction.

For a disk source, with one reference point $P(\mathbf{r}_1)$ fixed as in Fig. 3 we can calculate the coherence distribution as a function of $Q(\mathbf{r}_2)$. If $Q(\mathbf{r}_2)$ is on the Π_1 plane, the maximum coherence occurs at $P(\mathbf{r}_1)$ and decays like an Airy pattern. If $Q(\mathbf{r}_2)$ is not on the same plane as $P(\mathbf{r}_1)$ but is near Π_1, coherence is maximized if

$$v_{x_2} = (1 + \delta)v_{x_1}\,, \qquad v_{y_2} = (1 + \delta)v_{y_1}\,, \tag{12}$$

which we found by setting $B_x(0) = 0$ and $B_y(0) = 0$. We can see that near Π_1 the locus of points that are maximally coherent with $P(\mathbf{r}_1)$ is a line passing through the center of the disk source and through $P(\mathbf{r}_1)$ (Fig. 3). The modulus of the degree of coherence along that line is

$$|j(\mathbf{r}_1, \mathbf{r}_2)|_{\max} = \mathrm{sinc}\left(\frac{N_F}{2}\frac{\delta}{1 + \delta}\right). \tag{13}$$

Thus for $\delta \ll 1$ the upper limit of the coherence between two planes is a monotonic decreasing function of $N_F\delta$ or, equivalently, $(R/z_1)^2$. This result verifies the intuitive notion that if we want the illumination to be effectively incoherent we should use a large spinning disk or bring the illuminated object closer to the spinning disk. The exact contour of the coherence in the cross section at plane S is identical to Fig. 8.41 of Ref. 4. When $\delta \ll 1$, the coherence distribution is mirror symmetric with respect to plane Π_1 and rotationally symmetric about the line defined by Eqs. (12). From Fig. 3 we can also see that at distance $\delta = 1.5219/(N_F - 1.5219)$ away from Π_1 the locus branches into two segments. The reason for the branching is the peak-null configuration of $|\mathcal{L}()|$ (Fig. 8.41 of Ref. 4).

We now turn to the case of the thick cylinder, $\alpha > 0$. To get the locus of maximum coherence we maximize the slowly varying components $A(\xi)$ and $B(\xi)$ of the integrand by setting the arguments to $\mathcal{L}()$ equal to zero, which gives the same result as Eqs. (12), and we replace $C(\xi)$ with its Taylor expansion about $\xi = 0$:

$$C(\xi) \approx \frac{1}{4\pi^2}\frac{{v_1}^2}{N_F}\left[-\delta + 0\xi + \frac{\delta}{(1 + \delta)}\xi^2\right]. \tag{14}$$

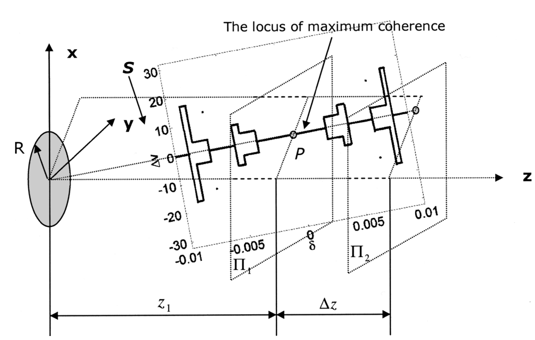

Fig. 3. Illustration of the coherence that originates from a quasi-monochromatic, spatially incoherent disk source: The parameters that we used to calculate the locus of maximum coherence are $\lambda = 488$ nm, $R = 5$ mm, and $\mathbf{r}_1 = (10, 10, 100 \text{ mm})$, which led to $N = 512.3$, $v_{x_1} = 6437.7$, and $v_{y_1} = 6437.7$.

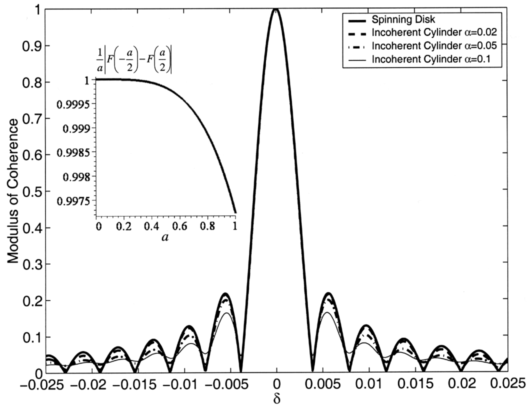

Fig. 4. Modulus of the degree of coherence along the line defined by Eqs. (12): The degree of coherence along the line is calculated for a disk source and three cylindrical sources with different values of α. The parameters used in the simulation were $N = 512.3$, $v_{x_1} = 6437.7$, and $v_{y_1} = 6437.7$.

The result is

$$|j(\mathbf{r}_1, \mathbf{r}_2)|_{\max} \approx \mathrm{sinc}\left(\frac{N_F}{2}\,\frac{\delta}{1+\delta}\right) \times \frac{1}{a}\left|F\left(-\frac{a}{2}\right) - F\left(\frac{a}{2}\right)\right|, \tag{15}$$

where

$$a = \alpha\left(\frac{1}{4\pi}\,\frac{{v_1}^2}{N_F}\,\frac{\delta}{1+\delta}\right)^{1/2} = \frac{L}{{z_1}^2}\left[\frac{\pi({x_1}^2 + {y_1}^2)\Delta z}{\lambda(1+\delta)}\right]^{1/2} \tag{16}$$

and $F()$ is the Fresnel integral.[4] Because of the weak dependence of the term $1/a|F(-a/2) - F(a/2)|$ on a (Fig. 4, inset), we can conclude that the effect of thickness on the degree of coherence along the line defined by Eqs. (12) is minimal. The exact effect of thickness on the maximal degree of coherence is shown in Fig. 4.

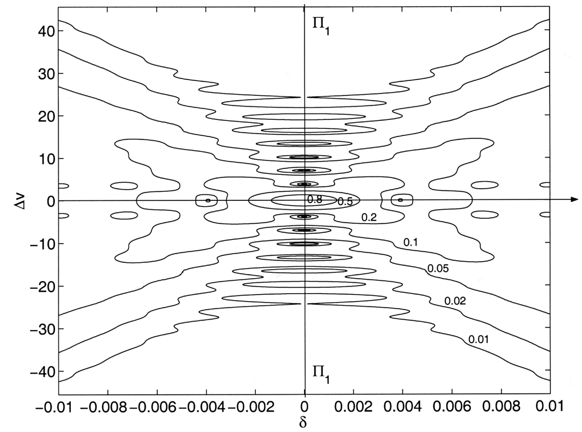

Fig. 5. Contour map of the coherence that originates from a cylindrical source in the cross section at plane S along the line defined by Eqs. (12): The parameters used in the simulation are the same as for Fig. 2.

The exact contour of the coherence in the cross section at plane S for a relatively thick cylinder is shown in Fig. 5. The distribution of coherence is not rotationally symmetric about the line given by Eqs. (12). Instead, it looks elliptical, similar to the diffraction pattern from volume holograms.

This research was supported by the U.S. Air Force Office of Scientific Research Multiuniversity Research Initiative (contract F49620-03-1-0320). We are grateful to Arnab Sinha and Wenyang Sun for helpful discussions. K. Tian's e-mail address is kehan@mit.edu.

References

1. L. Mandel and E. Wolf, *Optical Coherence and Quantum Optics* (Cambridge U. Press, Cambridge, 1995).
2. J. W. Goodman, *Statistical Optics* (Wiley, New York, 1985).
3. J. W. Goodman, *Introduction to Fourier Optics*, 2nd ed. (McGraw-Hill, New York, 1996).
4. M. Born and E. Wolf, *Principles of Optics*, 6th ed. (Pergamon, London, 1980).
5. H. Coufal, D. Psaltis, and G. Sincerbox, eds., *Holographic Data Storage* (Springer-Verlag, Berlin, 2000).